



ORIGINAL RESEARCH

Divergent paths to seizure-like events

Neela K. Codadu¹, Robert T. Graham¹, Richard J. Burman² , R. Thomas Jackson-Taylor¹, Joseph V. Raimondo² , Andrew J. Trevelyan¹ & R. Ryley Parrish¹ 

¹ Institute of Neuroscience, Medical School, Newcastle University, Newcastle upon Tyne, United Kingdom

² Division of Cell Biology, Department of Human Biology, Neuroscience Institute and Institute of Infectious Disease and Molecular Medicine, Faculty of Health Sciences, University of Cape Town, Cape Town, South Africa

Keywords

Epilepsy, ictal events, interneurons, interictal events.

Correspondence

R. Ryley Parrish and Andrew J. Trevelyan, Institute of Neuroscience, Medical School, Newcastle University, Newcastle upon Tyne, United Kingdom.

Tel: +44-191-208-5732

E-mails: ryley.parrish@ncl.ac.uk;

andrew.trevelyan@ncl.ac.uk

Funding information

The work was supported by project grants from Epilepsy Research UK (P1504) and Medical Research Council (UK) (MR/J013250/1 and MR/R005427/1).

Received: 7 June 2019; Revised: 29 July 2019; Accepted: 31 July 2019

doi: 10.14814/phy2.14226

Physiol Rep, 7 (19), 2019, e14226,
<https://doi.org/10.14814/phy2.14226>

Introduction

Understanding how seizures develop and spread although cortical tissue is of great clinical importance. About 65 million people worldwide are diagnosed as having epilepsy, and many others will experience a seizure at some point in their life (Jacoby and Baker, 2008; Sirven, 2015). There remain, however, many unresolved issues regarding the basic mechanisms leading to a seizure. Efforts to derive overarching principles regarding epileptic pathophysiology must take into account the key differences between patient phenotypes or between experimental models. Early studies of disinhibited networks showed that, without GABAergic restraint, epileptic discharges could be entrained from single neurons (Miles and Wong,

Abstract

Much debate exists about how the brain transitions into an epileptic seizure. One source of confusion is that there are likely to be critical differences between experimental seizure models. To address this, we have compared the evolving activity patterns in two widely used in vitro models of epileptic discharges. Brain slices from young adult mice were prepared in the same way and bathed either in 0 Mg²⁺ or 100 μmol/L 4AP artificial cerebrospinal fluid. We have found that while local field potential recordings of epileptiform discharges in the two models appear broadly similar, patch-clamp analysis reveals an important difference in the relative degree of glutamatergic involvement. 4AP affects parvalbumin-expressing interneurons more than other cortical populations, destabilizing their resting state and inducing spontaneous bursting behavior. Consequently, the most prominent pattern of transient discharge (“interictal event”) in this model is almost purely GABAergic, although the transition to seizure-like events (SLEs) involves pyramidal recruitment. In contrast, interictal discharges in 0 Mg²⁺ are only maintained by a very large glutamatergic component that also involves transient discharges of the interneurons. Seizure-like events in 0 Mg²⁺ have significantly higher power in the high gamma frequency band (60–120Hz) than these events do in 4AP, and are greatly delayed in onset by diazepam, unlike 4AP events. We, therefore, conclude that the 0 Mg²⁺ and 4AP models display fundamentally different levels of glutamatergic drive, demonstrating how ostensibly similar pathological discharges can arise from different sources. We contend that similar interpretative issues will also be relevant to clinical practice.

1983). This work further provided a detailed, ionic model of the paroxysmal depolarising shift (Traub and Miles, 1991). The disinhibition models show what can happen with a deficit of GABAergic activity, but cannot address how interneuronal activity might shape epileptic activity. Interneuronal function, on the other hand, has been a dominant theme in studies where epileptic activity is induced either by bathing the tissue in 0 Mg²⁺ (Anderson et al., 1986; Mody et al., 1987; Wong and Prince, 1990) or in 4-aminopyridine (4AP) (Buckle and Haas, 1982; Rutecki et al., 1987; Avoli et al., 2002) ACSF.

In the 0 Mg²⁺ model, the primary cellular effect is to remove the voltage-dependent blockade of NMDA receptors (Mayer et al., 1984), thereby greatly enhancing the postsynaptic effect of any glutamatergic synaptic inputs

(Mayer et al., 1984). In contrast, the primary effect of 4AP is to block certain classes of voltage-dependent K^+ channels. In both cases, the direct pharmacological actions occur rapidly (seconds to minutes), and yet epileptiform activity evolves on a rather slower timescale, over many minutes to hours, suggestive that there are emergent network alterations in each model that are critical for ictogenesis. An added appeal of the 4AP model is that it can be applied *in vivo* (Fragoso-Veloz and Tapia, 1992; Martin and Pozo, 2003; Levesque et al., 2013), producing ostensibly similar discharges to the *in vitro* activity patterns. Both *in vivo* and *in vitro* 4AP models have been used to good effect in tandem with optogenetic stimulation of specific subpopulations of neurons, indicating how in this special case, interneurons may drive ictogenesis (Shiri et al., 2015; Yekhle et al., 2015; Chang et al., 2018; Magloire et al., 2018). This is hypothesized to happen through a sequence involving chloride-loading of pyramidal cells and secondary rises in extracellular K^+ via the potassium chloride cotransporter (KCC2) (Viitanen et al., 2010; Gonzalez et al., 2018; de Curtis et al., 2019; Schevon et al., 2019).

In contrast, the 0 Mg^{2+} model can only be used *in vitro* (it is harder to remove ions than it is to add a drug), but it, too, involves intense bursts of interneuronal activity (Trevelyan et al., 2006; Trevelyan et al., 2007; Parrish et al., 2019), and evidence of short-term changes in GABAergic function (Ellender et al., 2014; Raimondo et al., 2015), although, unlike the 4AP model, the interneuronal activity initially appears to act as a restraint on the spreading epileptiform discharges (Trevelyan and Schevon, 2013; Trevelyan, 2016). It is important to resolve these two contrasting views of the role of the interneuronal bursting. We hypothesized that the explanation may lie in the level of concurrent glutamatergic drive in the two models. We therefore made a detailed comparison of activity patterns in these two models, using brain slices prepared in the same way from young adult mice.

Methods

Ethical approval

All animal handling and experimentation were done according to the guidelines laid by the UK Home Office and Animals (Scientific Procedures) Act 1986 and approved by the Newcastle University Animal Welfare and Ethical Review Body (AWERB # 545).

Slice preparation

Male and female Emx1-Cre (B6.129S2-Emx1tm1(cre)Krl/J; Jackson Laboratory stock number 5628), PV-Cre

(B6;129P2-Pvalb < tm1(cre)Arbr>/J; Jackson Laboratory stock number 8069), and SOM-Cre (B6N.Cg.Ssttm2.1(cre)Zjh/J; Jackson Laboratory stock number 18973) mice and C57/B6 mice (ages 3–12 weeks) were used in this study. Transgenic mice were back-crossed with the C57/B6 line maintained at Newcastle University, and subsequently maintained on this C57/B6 background (Jackson Laboratory stock number 000664). Mice were housed in individually ventilated cages in 12 h light, 12 h dark lighting regime. Animals received food and water *ad libitum*. Mice were sacrificed by cervical dislocation, brains removed and stored in cold cutting solution (in mM): 3 MgCl_2 ; 126 NaCl ; 26 NaHCO_3 ; 3.5 KCl ; 1.26 NaH_2PO_4 ; 10 glucose. For local field potential (LFP) recordings, 400 μm horizontal sections were made, using a Leica VT1200 vibratome (Nussloch, Germany). Slices were then transferred to an interface holding chamber and incubated for 1–2 h at room temperature in artificial CSF (ACSF) containing (in mM): 2 CaCl_2 ; 1 MgCl_2 ; 126 NaCl ; 26 NaHCO_3 ; 3.5 KCl ; 1.26 NaH_2PO_4 ; 10 glucose. For patch clamp experiments, coronal sections were made at 350 μm , and stored in a submerged holding chamber for 1–4 h prior to experimentation. All the solutions were bubbled continuously to saturate with carboxygen (95% O_2 and 5% CO_2).

Extracellular field recordings were performed using interface recording chambers. Slices were placed in the recording chamber perfused with modified artificial cerebrospinal fluid (ACSF) to induce epileptiform activity (0 Mg^{2+} or 100 $\mu\text{mol/L}$ 4-aminopyrimidine). Recordings were obtained using normal ACSF-filled 1–3 $\text{M}\Omega$ borosilicate glass microelectrodes (GC120TF-10; Harvard Apparatus, Cambridge, UK) placed in deep layers of the temporal association area. Experiments were performed at 33–36°C. The solutions were perfused at the rate of 3.5 mL/min . Waveform signals were acquired using BMA-931 biopotential amplifier (Dataq Instruments, Akron, OH, USA), Micro 1401-3 ADC board (Cambridge Electronic Design, Cambridge, UK) and Spike2 software (v7.10, Cambridge Electronic Design). Signals were sampled at 10kHz, amplified (gain: 500) and bandpass filtered (1–3000Hz). CED4001-16 Mains Pulser (Cambridge Electronic Design) was connected to the events input of CED micro 1401-3 ADC board and is used to remove 50Hz hum offline. SLEs were visually identified with their start time as the time of occurrence of high-frequency rhythmic bursts (tonic-phase) associated with high-frequency signals, and the events were considered to end when the interval between two after-discharges (clonic-phase) is $\geq 2\text{s}$. Frequency analysis of the recordings was performed using a custom-written code in Matlab2018b (MathWorks, Natick, MA, USA).

Viral injections

PV-Cre and SOM-Cre, or Emx1-Cre pups were injected with AAV5.Syn.Flex.tdTomato, purchased from the University of Pennsylvania vector core. Injections were performed either on the day of birth, or the following day. Pups were set on a stereotaxic frame and anesthetized with isoflurane, following application of EMLA cream (2.5% lidocaine and 2.5% prilocaine) to the left top of their head. Injections were made, using a 10 μ L Hamilton syringes with a bevelled 36-gauge needle (World Precision Instruments, Sarasota, FL, USA), unilaterally into the lateral ventricle and overlying cortical plate, at about 1 mm anterior to lambda and 1 mm lateral to the midline into the left hemisphere, starting at 1.7 mm deep from the top of the dura mater, for a total of four separate 50 nL injections, deepest first and coming up 0.3 mm for each subsequent injection. Approximately 200 nL (\sim 1000 viral particles) were injected into the left hemisphere over a 10-min period. Pups were monitored until they awoke following the procedure and then returned to their home cage. These neonatal injections produced widespread cortical expression of tdTomato into the neurons of interest.

Patch-clamp recordings

Slices were perfused at 3–5 mL/min and heated to 33–34°C. Whole cell data were acquired using pClamp software, Multiclamp 700B, and Digidata acquisition board (Molecular Devices, Sunnyvale, CA, USA). Whole cell recordings of layer five neurons from the temporal association area were made using 4–7 M Ω pipettes. Pipettes were filled with a KMeSO₄-based internal solution containing (mM): 125 KMeSO₄, 6 NaCl, 10 HEPES, 2.5 Mg-ATP, 0.3 Na₂-GTP. For the voltage clamp recordings, 5 mmol/L QX-314 (N-(2,6-dimethylphenylcarbonylmethyl) was added to the internal solution to block action potential firing while the cells were held at -30 mV. Osmolarity and pH of all the internal solutions used were adjusted to 284mOsm and 7.4. The targeted patch experiments of the PV-interneurons, SST-interneurons, and pyramidal neurons were done in current clamp mode, with the cells being identified by the presence of tdTomato. The fluorescence was visualized using an Olympus DSU spinning disk BX/50WI upright microscope (UMPlanFL N 20x, 0.5 NA objective; Olympus, UK), illuminated using a Mercury arc lamp, controlled with a fast Sutter shutter (Sutter Instrument, USA), using the standard Olympus rhodamine (UMRFPHQ) filter set. The system utilizes a Hamamatsu C9100 EM camera (Hamamatsu Photonics, Japan) to collect images, run by Simple PCI software (Digital Pixel, UK) installed on Dell Precision computers (Dell, UK).

Patch clamp data were analyzed using custom-written codes in Matlab2018b. Briefly, epileptiform discharges were identified from the voltage clamp recordings and classified automatically. In short, the events immediately prior to seizures, occurring at \sim 1–2Hz, and progressing straight into a full SLE, are referred to as “preictal events”. Other transient discharges (<500 msec duration) which occur at a much lower rate (\sim 0.1Hz) are referred to as “interictal events” (note that these also include events prior to the first SLE, even though as such, these events are not “inter”-ictal). Trace deflections fitting a generalised model were grouped by their structure as excitatory only, inhibitory only. All events were considered for the composite category and were recategorized only if they displayed bidirectional deflections with respect to a dynamically calculated baseline.

Pharmacology

Drugs acting at glutamatergic and GABAergic receptors were used at the following concentrations: 50 μ mol/L D-2-amino-5-phosphonovalerate (AP5) (Hello Bio, Bristol, UK); 20 μ mol/L NBQX disodium salt (Hello Bio, Bristol, UK); 10 μ mol/L Gabazine (Hello Bio, Bristol, UK); 3 μ mol/L Diazepam (Tocris, Abingdon, UK); 5 μ mol/L CGP-55845 (Hello Bio, Bristol, UK).

Data analysis and statistics

Data were analyzed offline using Matlab R2018b (MathWorks, USA). Groups of two were analyzed using the Mann–Whitney test or Student’s *t*-test. A Kruskal–Wallis test followed by a Dunn’s multiple comparison test was used for data with 3 or more groups. Proportion data were analyzed with a Chi-square test. Significance was set at $P \leq 0.05$ for all analyses. Data represented as mean \pm SEM unless otherwise mentioned.

Results

Superficial similarities between 0 Mg²⁺ and 4AP-induced epileptiform activity

Brain slice preparations have long been used to understand how epileptic discharges are manifest in cortical networks. We compared the neocortical activity patterns that occur in two widely used models, induced by bathing brain slices in either 0 Mg²⁺ or 100 μ mol/L 4-aminopyridine (4AP) artificial cerebrospinal fluid (ACSF). Both models induce an evolving pattern of interictal and seizure-like activity, in neocortex, eventually progressing into a pattern of rhythmic epileptiform discharges, termed late recurrent discharges (LRDs), that has been likened to

status epilepticus (Fig. 1, Ai, Aii) (Anderson et al., 1986; Dreier and Heinemann, 1991). The times to the first full ictal event, and to the LRD, in 4AP are significantly shorter than in 0 Mg^{2+} but otherwise, the activity patterns appear broadly similar (Fig. 1B–E).

Extracellular recordings, however, are rather abstracted representations of the underlying activity, and so while they clearly have a large informational content, the underlying neuronal causes of the signal often remains rather cryptic. We therefore explored the two models using patch-clamp recordings of pyramidal cells (Fig. 2). Large, layer five pyramidal cells have dendritic trees that extend through the full depth of the cortex, meaning that recordings from these cells provide a good sampling of synaptic drives onto a cortical column. We recorded 19 pyramidal cells (10 cells in 0 Mg^{2+} ; 9 cells in 4AP) in voltage clamp, holding the cells at -30 mV , roughly halfway between the reversal potential of glutamatergic and GABAergic receptors. This approach had previously proved highly informative about the pattern of synaptic bombardment

during spreading ictal events (Trevelyan et al., 2006). In 4AP, most early interictal-like discharges were manifest as entirely upward deflections, suggestive of an overwhelming preponderance of GABAergic activity. In contrast, the majority of 0 Mg^{2+} events showed prominent downward deflections, indicative of large glutamatergic drive. The two models were highly significantly different (Fig. 2Aii, Bii). These same patterns were replicated in the events immediately prior to ictal events (pre-ictal activity; Fig. 3Ai, Bi), and which likewise showed a highly significant difference in the level of glutamatergic drive in the two models (Fig. 3Aii, Bii). Taken together, these data demonstrate that despite the ostensible LFP similarities, there are important differences between the models, particularly in the pattern of synaptic drive onto the pyramidal cell population, suggesting that different cell populations may drive the generation of pathological discharges in the two models.

We next examined the source of the ictal-like activity through pharmacological dissection of the glutamatergic

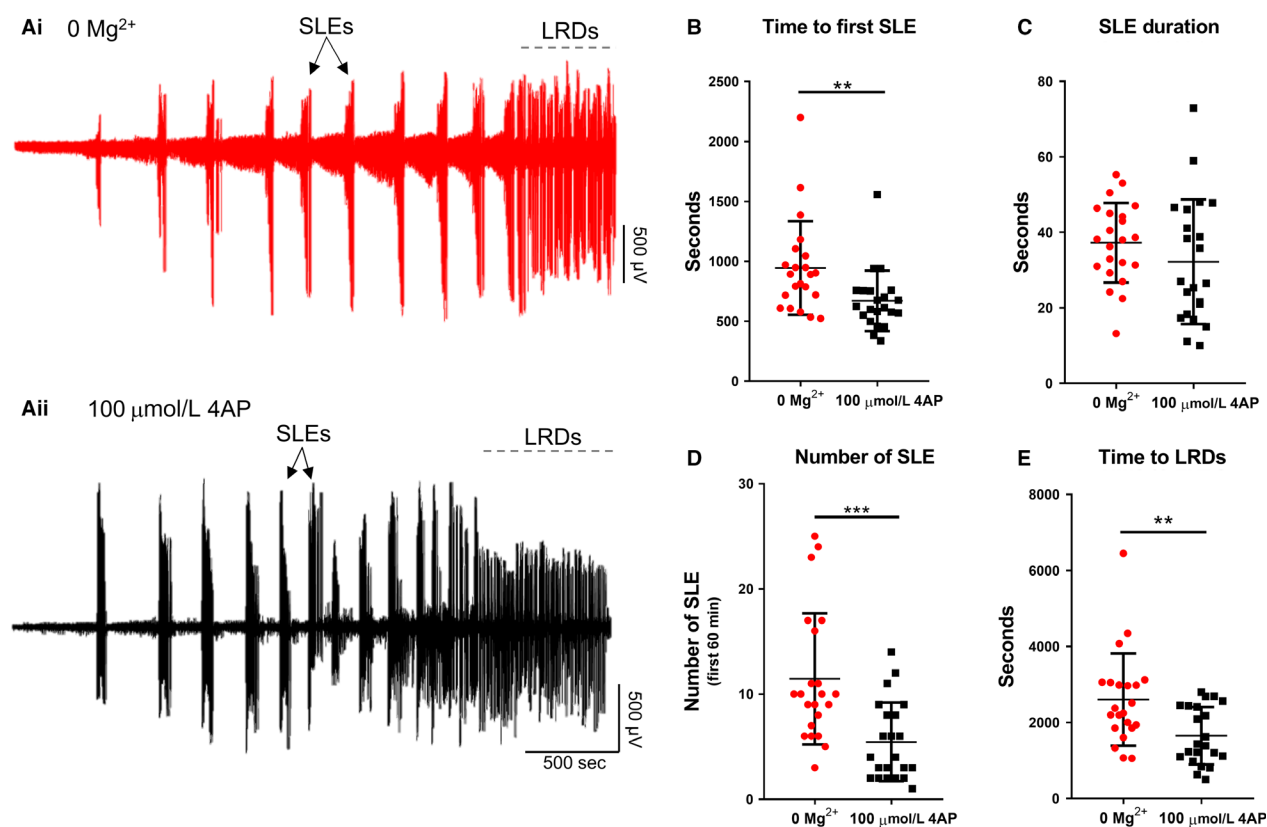


Figure 1. Similarities between evolving epileptiform activity, in 0 Mg^{2+} and 4AP ACSF. (Ai) Example trace from 0 Mg^{2+} -induced epileptiform activity. (Aii) Equivalent recording in 4AP. (B) The 4AP model leads to SLE significantly faster than the 0 Mg^{2+} model (Mann–Whitney test, $**P = 0.0017$). (C) There is no difference between the duration of seizures between the 4AP and 0 Mg^{2+} models (Mann–Whitney test, $P = 0.1733$). (D) There is a significant difference in the number of SLE between the 4AP and 0 Mg^{2+} models (Mann–Whitney test, $***P = 0.0002$). (E) The 4AP model enters LRD significantly earlier than the 0 Mg^{2+} model (Mann–Whitney test, $**P = 0.005$).

and GABAergic components of the network. As expected, application of AMPA and NMDA receptor blockers resulted in the abolishment of all interictal and ictal-like activity in the 0 Mg^{2+} model (Fig. 4A). In contrast, in the 4AP model, application of glutamate receptor blockers only blocked the ictal-like activity, but interictal activity persisted, as has been previously reported (Avoli *et al.*, 2002; Bohannon and Hablitz, 2018). This interictal activity was eliminated through the application of the of GABA_A receptor blocker gabazine (Fig. 4B), strongly suggesting that this remaining epileptiform activity is due to inhibitory post-synaptic currents (IPSCs) onto the pyramidal cells (Avoli *et al.*, 2002). This demonstrates that while seizure-like events in both models are downstream of glutamate receptor activation, the source of the interictal activity is fundamentally different between the two models.

4AP preferentially activates PV interneurons

In order to understand the source of the persistent epileptiform activity in the 4AP model, we examined

the direct effects of 4AP on firing patterns in the three main classes of neocortical neurons: pyramidal cells, and both parvalbumin-expressing (PV), and somatostatin-expressing (SST) interneurons. Recordings were performed in the absence of any fast synaptic neurotransmission (glutamatergic blockade: $20 \mu\text{mol/L}$ NBQX and $50 \mu\text{M}$ AP5; GABAergic blockade: $10 \mu\text{mol/L}$ gabazine and $5 \mu\text{mol/L}$ CGP-55845). 4AP induced spontaneous action potential firing in all cell classes studied (Fig. 5A), but the effect on PV-interneurons was larger than on the other two cell classes (Fig. 5B). Consistent with this finding, 4AP application had no appreciable effect on the resting membrane potential, or input resistance, of either pyramidal cells or SST interneurons, but it induced a highly significant increase in the input resistance of PV interneurons (Table 1). Additionally, 4AP reduced action potential threshold in both PV and pyramidal cells (but not SST interneurons), but this only translated into an increase in the evoked firing (triggered by a 100 pA current injection) in PV interneurons, but not in the pyramidal cells (Table 1; Fig. 5D; 6B).

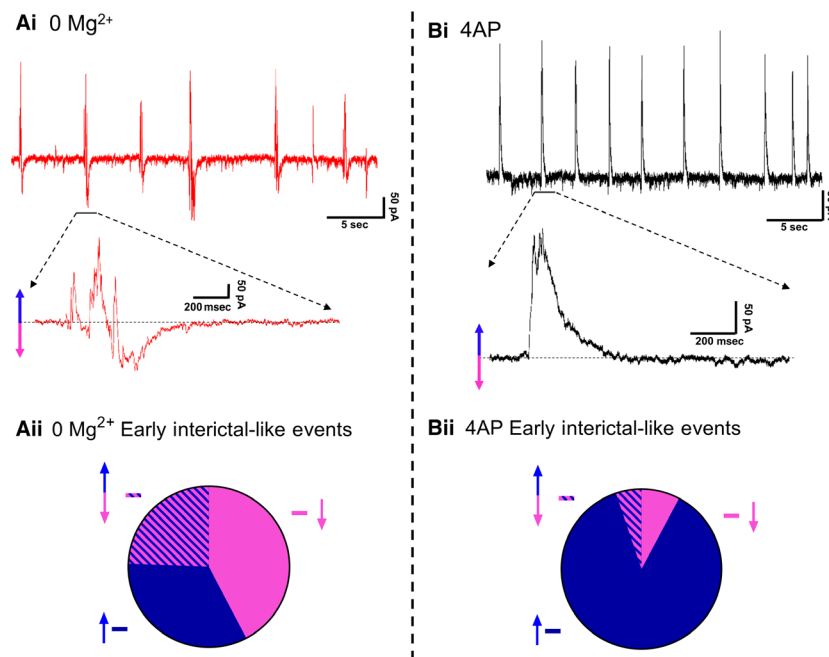


Figure 2. Different levels of glutamatergic drive in early interictal-like events, in the two models. (Ai) Example patch-clamp recording of typical early interictal-like events onto a layer 5 pyramidal cell induced by washout of Mg^{2+} ions (Cell is being held at -30 mV). (Aii) Pie chart demonstrating the proportion of putative IPSCs (33.3%, represented with an upward blue arrow), EPSCs (42.3%, represented with a downward pink arrow), and composite events (events containing both a putative IPSC and an EPSC; 24.4%, represented with both an upward blue arrow and a downward pink arrow) of early interictal-like postsynaptic currents onto pyramidal cells after washout of Mg^{2+} ions (4002 events were analyzed from 10 slices). (Bi) Equivalent recording in 4AP as shown in Ai (Cell is being held at -30 mV). (Bii) Pie chart demonstrating the proportion of putative IPSCs (87.0%, represented with an upward blue arrow), EPSCs (7.8%, represented with a downward pink arrow), and composite events (5.2%, represented with both an upward blue arrow and a downward pink arrow) of early interictal-like postsynaptic currents onto pyramidal cells after addition of 4AP (9992 events were analyzed from nine slices, Proportion data from 4AP is significantly different from the 0 Mg^{2+} paradigm, χ^2 test, $P < 0.0001$).

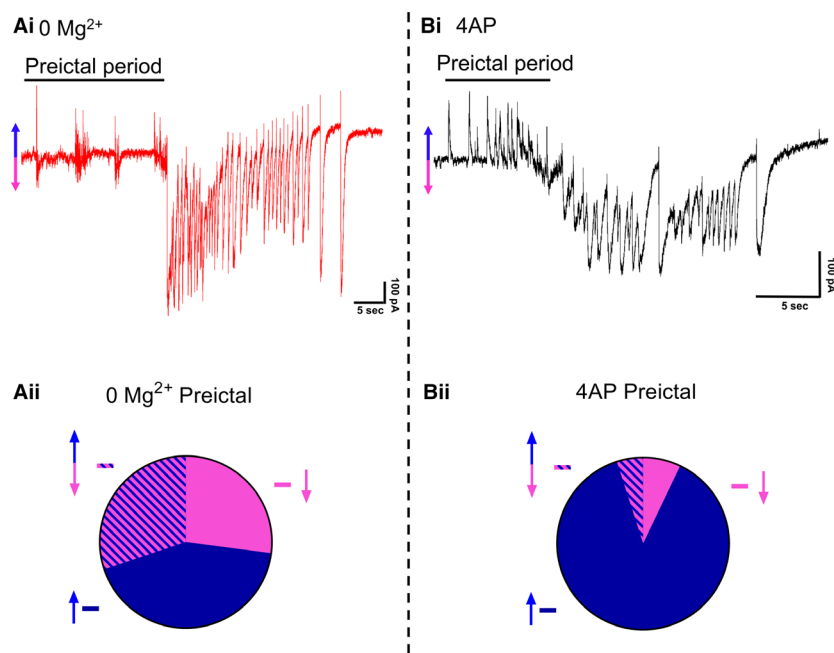


Figure 3. Different levels of glutamatergic drive during preictal activity, in the two models. (Ai) Example patch-clamp recording of typical SLE induced by washout of Mg^{2+} ions (Cell is being held at -30 mV). (Aii) Pie chart demonstrating the proportion of putative IPSCs (42.8%, represented with an upward blue arrow), EPSCs (27.0%, represented with a downward pink arrow), and composite events (events containing both a putative IPSC and an EPSC; 30.2%, represented with both an upward blue arrow and a downward pink arrow) of preictal postsynaptic currents onto pyramidal cells after washout of Mg^{2+} (152 events were analyzed from 10 slices). (Bi) Equivalent recordings in 4AP as shown in Ai (Cell is being held at -30 mV). (Bii) Pie chart demonstrating the proportion of putative IPSCs (88.0%, represented with an upward blue arrow), EPSCs (7.0%, represented with a downward pink arrow), and composite events (5.0%, represented with both an upward blue arrow and a downward pink arrow) of preictal postsynaptic currents onto pyramidal cells after addition of 4AP (105 events were analyzed from 9 slices, Proportion data from 4AP is significantly different from the 0 Mg^{2+} paradigm, χ^2 test, $P < 0.0001$).

4AP further caused a highly significant broadening of action potentials in all cell classes, although the effect was much larger in the interneuronal classes (84% and

104% increase in PV and SST interneurons, respectively, but only 18% increase for pyramidal cells, Fig. 6A; Table 1), confirming a previous report that 4AP can

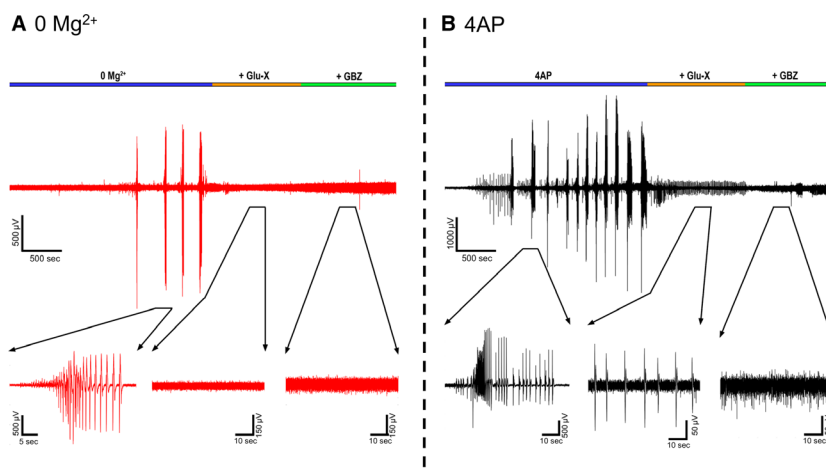


Figure 4. 4AP interictal-like activity is sustained in the presence of glutamatergic blockers but not in the 0 Mg^{2+} paradigm. (A) Representative LFP trace of a 0 Mg^{2+} recording before and after addition of Glu-X (NBQX and AP5) and Glu-X plus Gabazine ($N = 3$). (B) Equivalent recordings in 4AP ($N = 3$).

cause a broadening of neuronal action potentials (Mittendorfer and Bean, 2002).

We concluded that 4AP affects PV-interneuron firing more than it does SST and pyramidal firing, leading to a preferential activation of the PV cell class, supporting previous findings which were not performed in the blockade of both glutamatergic and GABAergic currents (Williams and Hablitz, 2015). PV interneurons are, thus, likely to be the main source of the persistent pathological discharges following application of glutamate receptor blockers, in this model. We therefore performed targeted, cell-attached patch clamp recordings of the PV interneuron population during spontaneous interictal events in the two models (no glutamatergic blockade). We found that while the mean and maximal firing rates during these interictal bursts were comparable in the two models, these bursts of firing lasted approximately twice as long in the 4AP events and comprised roughly three times as many action potentials per event (Fig. 7).

We next analyzed prolonged extracellular recordings of 22 brain slices bathed in 4AP and 24 slices bathed in 0 Mg^{2+} , to investigate whether the difference in glutamatergic involvement between the models was evident in the local field potential. To control for differences in the electrode quality, we normalized the traces to the maximal

field deflection during full ictal events, since we reasoned that these are likely to reflect comparable levels of network activation in the two models. In each model, in almost identical proportions, we found instances of both low voltage, fast onset, (0 Mg^{2+} model, 43% of events; 4AP model, 44% of events), and hypersynchronous onset (0 Mg^{2+} model, 57% of events; 4AP model, 56% of events). A power spectra analysis over the entire ictal events indicated that there was a significant excess power at frequencies in the high gamma range in the 0 Mg^{2+} (Fig. 8). This excess power observed in the 0 Mg^{2+} model extended also into the fast ripple range (250 to 500 Hz, data not shown). Another notable difference between the models is that the post-ictal refractory period lasted far longer in 0 Mg^{2+} (time delay after the first seizure, before the resumption of interictal discharges = 106.2 ± 13.6 s; $n = 24$ brain slices) compared with that in 4-AP (post-ictal delay = 24.9 ± 10.6 s; $n = 22$; $P = 3.0e-5$).

The 0 Mg^{2+} and 4AP models differ in their sensitivity to diazepam.

Finally, we examined whether there were differences in sensitivity to the benzodiazepine family of drugs between the models as a result of their different drives. We found

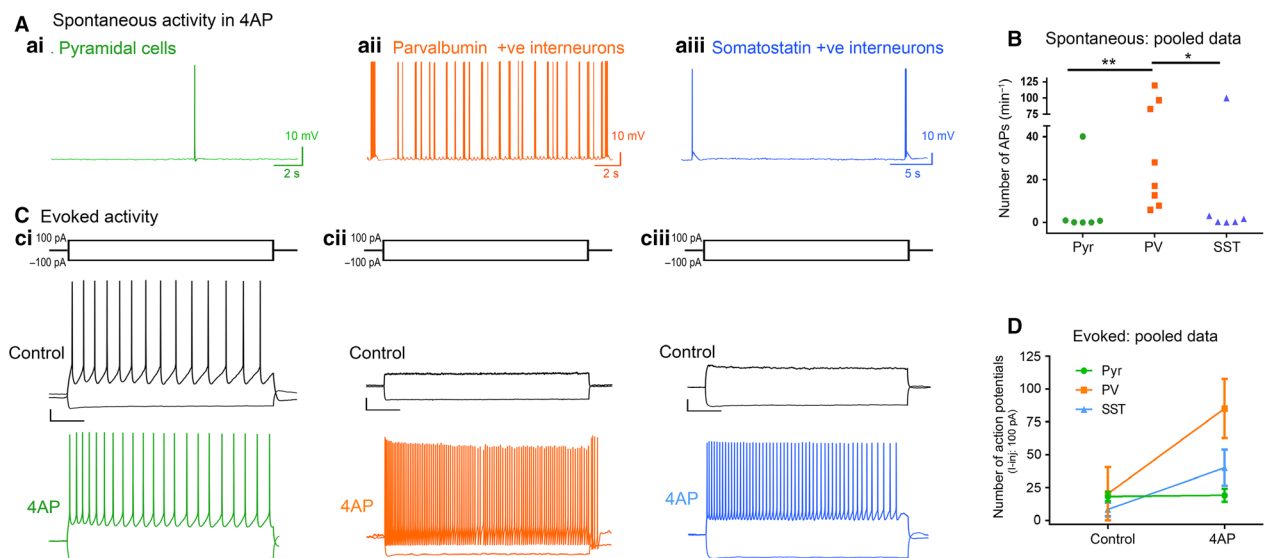


Figure 5. 4AP preferentially induces increased action potential firing in the PV cell population compared to pyramidal and SST cells. (A) Spontaneous activity: representative traces of a pyramidal cell, a PV-interneuron, and a SST-interneuron following wash in of 100 μ mol/L 4AP with Glutamate (NBQX and AP5) and GABA (Gabazine and CGP-55845) receptor blockers ($N = 6$). (B) Spontaneous action potential firing in the PV cells is significantly higher than in the pyramidal or SST cells (Kruskal–Wallis Test with post hoc test, $**P = 0.008$ for pyramidal vs PV, $*p = 0.042$ for SST vs PV). (C) Evoked activity: representative traces showing responses of (Ci) a pyramidal cell, (Cii) a PV interneuron, and (Ciii) a SST interneuron to 3s long hyperpolarisation (-100 pA) and depolarization (100pA) current pulses, in the presence of 4AP (GABA and glutamatergic neurotransmission blocked). Scale bars: horizontal, 500 ms; vertical, 10 mV. (D) 4AP increased the number of action potentials fired by PV interneurons (Wilcoxon matched-pairs rank test, $P = 0.008$; $N = 9$) in response to 100pA current injection, but not by pyramidal cells (paired t -test, $P = 0.769$; $N = 6$) or SST interneurons (Wilcoxon matched-pairs rank test, $P = 0.125$; $N = 6$).

Table 1. Cellular electrophysiological attributes, measured in control media and in 4AP (ns, not significant; * $p < 0.05$; ** $p < 0.01$)

	Control	4AP	% change	P-value	
Parvalbumin positive interneuron ($n = 9$)					
Resting Em (mV)	-63.8 ± 2.1	-62.4 ± 2.5	-2.2	0.205	ns
Rin ($M\Omega$)	114.5 ± 11.9	131.7 ± 12.1	15.5	0.002	**
AP threshold (mV)	-39.1 ± 1.8	-45.1 ± 2.6	15.3	0.021	*
AP threshold (mV) relative to Em	24.8 ± 3.3	17.5 ± 4.3	-29.4	0.014	*
Half-width (ms)	0.37 ± 0.02	0.68 ± 0.02	83.8	<0.001	**
Somatostatin positive interneuron ($n = 6$)					
Resting Em (mV)	-64.6 ± 1.9	-63.9 ± 2.3	-1.1	0.671	ns
Rin ($M\Omega$)	224.9 ± 48.4	251.5 ± 51.2	11.8	0.057	ns
AP threshold (mV)	-41.4 ± 1.5	-45.9 ± 1.8	10.9	0.158	ns
AP threshold (mV) relative to Em	23.1 ± 2.9	18.1 ± 2.1	-21.6	0.233	ns
Half-width (ms)	0.52 ± 0.05	1.06 ± 0.12	103.8	0.002	**
Pyramidal cell ($n = 6$)					
Resting Em (mV)	-72.2 ± 1.8	-75.3 ± 3.4	4.3	0.374	ns
Rin ($M\Omega$)	163.1 ± 23.6	176.1 ± 17.3	8.0	0.418	ns
AP threshold (mV)	-44.8 ± 3.4	-56.1 ± 4.4	25.2	0.023	*
AP threshold (mV) relative to Em	27.4 ± 1.8	19.3 ± 2.4	-29.6	0.02	*
Half-width (msec)	1.09 ± 0.09	1.29 ± 0.13	18.3	0.033	*

that bath application of diazepam significantly delayed the onset of the SLE and increased the duration of the early interictal period in the 0 Mg^{2+} model, while having no effect in the 4AP model (Fig. 9A–D). Additionally, in the 0 Mg^{2+} model, the number and rate of early interictal-like events were greatly increased by diazepam. In contrast, diazepam affected neither in 4AP (Fig. 9E and F). These data further suggest that these models produce epileptiform activity by different mechanisms and serve to illustrate how important it is to understand the source of epileptiform activity, when considering how to manage it.

Discussion

In this study, we made side-by-side comparisons of *in vitro* epileptiform activity induced either by bathing in 0 Mg^{2+} ACSF, or in $100 \mu\text{M}$ 4AP. Brain slices were prepared in the same way (often from the same animals), from young-adult mice. These two models have provided many insights into the basic pathophysiology of epilepsy, but critically for this debate, the two models differ in important ways, and yet there are frustratingly few direct comparisons of these. We showed previously that the two models affect hippocampal and neocortical areas differently (Codadu et al., 2019) (note that the entorhinal cortex appears to align with neocortical activity, rather than the hippocampal circuitry, in this regard), with the hippocampal territories being activated early in 4AP, but very late in 0 Mg^{2+} . Here, we focused on neocortical activity patterns, and showed that 4AP has an especially strong effect on PV-expressing interneurons (although it also alters, to a

lesser extent, activity in both SST-expressing interneurons and pyramidal cells), triggering spontaneous bursting in these cells (consistent with a previous report (Williams and Hablitz, 2015)). These bursts are readily apparent as isolated short-lasting (<1s) discharges in the LFP. Similar duration discharges are also seen in 0 Mg^{2+} ACSF, and both are commonly referred to by the same term, “interictal events” and we have shown previously that these interictal events involve PV cell firing in both models (Parrish et al., 2018). A more detailed examination using patch-clamp recordings of pyramidal cells, however, reveal a notable difference between these discharges: the 4AP events are almost purely inhibitory, whereas the 0 Mg^{2+} events also have a large glutamatergic component. This difference is also apparent in the preictal bursts.

It has been reported, previously, that the 4AP *in vitro* model induces low voltage fast onset seizure types (Shiri et al., 2015). We therefore investigated whether the two models showed different onset patterns, but found instead that both models displayed the low voltage fast onset pattern about 50% of the time, and were just as likely to display a hypersynchronous onset pattern. The variability may be in the proximity to the “ictal focus” within the slice, such that some recordings are of the ictogenic process, whereas others are of the secondary generalization, but the key point is that both models show this heterogeneity. 0 Mg^{2+} seizure-like events showed significantly higher power at frequencies above 60Hz, and far more protracted post-ictal suppression, relative to 4AP events. Indeed, in many slices bathed in 4AP, the interictal discharges resume almost immediately.

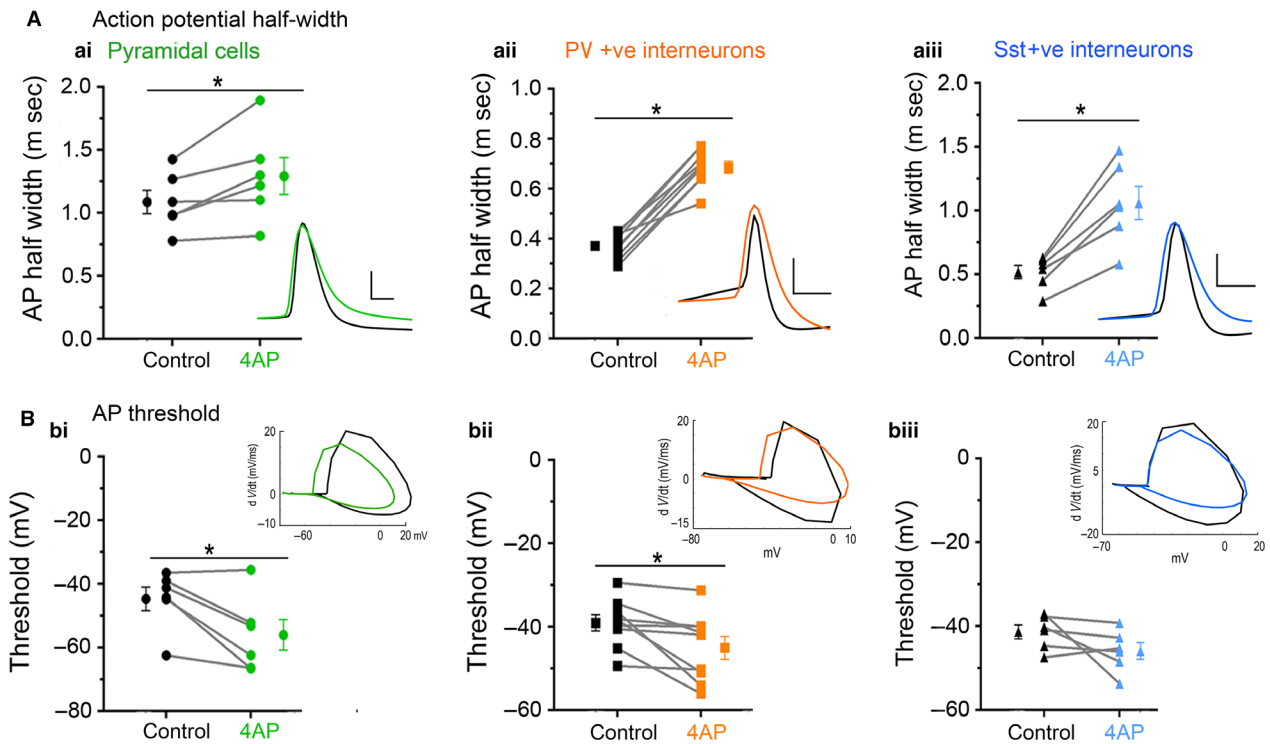


Figure 6. 4AP affects the firing properties in both PV- and SST-expressing interneurons, and also pyramidal cells. (Ai) 4AP significantly increased the action potential half-width of pyramidal cells (paired *t*-test, $P = 0.033$; $N = 6$). Inset: representative pyramidal cell action potential trace before (black) and after (green) 4AP. Scale bars: horizontal, 1 ms; vertical, 20 mV. (Aii) 4AP significantly increased the action potential half-width of PV interneurons (paired *t*-test, $P < 0.0001$; $N = 9$). Inset: representative PV interneuron action potential trace before (black) and after (orange) 4AP. Scale bars: horizontal, 1ms; vertical, 20 mV. (Aiii) 4AP significantly increased the action potential half-width of SST interneurons (paired *t*-test, $P = 0.002$; $N = 6$). Inset: representative SST interneuron action potential trace before (black) and after (blue) 4AP. Scale bars: horizontal, 1ms; vertical, 20 mV. (Bi) 4AP significantly reduced the action potential threshold of pyramidal cells (paired *t*-test, $P = 0.023$; $N = 6$). Inset: representative phase plots of pyramidal cell action potential trace before (black) and after (green) 4AP. (Bii) 4AP significantly reduced the action potential threshold of PV interneuron (paired *t*-test, $P = 0.021$; $N = 9$). Inset: representative phase plots of PV interneuron action potential trace before (black) and after (orange) 4AP. (Biii) 4AP had no effect on the action potential threshold of SST interneuron (paired *t*-test, $P = 0.159$; $N = 6$). Inset: representative phase plots of SST interneuron action potential trace before (black) and after (blue) 4AP.

We also found a marked difference in the drug sensitivity of the two models: benzodiazepines (Fig. 9) have little effect on the evolving activity in 4AP, but markedly reduce the early activity and the time to first seizure-like events in 0 Mg^{2+} . Consistent with this, other groups have noted that persistent epileptiform bursting leads to a reduced sensitivity of neurons to diazepam (Kapur and Macdonald, 1997; Dreier *et al.*, 1998; Goodkin *et al.*, 2005; Burman *et al.*, 2019). Notably, previous work showed that gap-junction blockers also affect the two models differently, giving mixed results appearing to enhance (Voss *et al.*, 2009) activity in 0 Mg^{2+} , but suppressing 4AP-induced activity (Chang *et al.*, 2013; Manjarrez-Marmolejo and Franco-Perez, 2016).

Our studies have focused on neuronal activity, but the two models are also likely to differ in respect to the involvement of glia. 4-AP, at the concentration used here

and in many other studies of epileptiform activity, has been shown to block completely a slowly inactivating K^+ channel in glia, and at higher concentrations (2–8 mmol/L), progressively also block all the other glial voltage-gated K^+ channels (Bordey and Sontheimer, 1999). This might be expected to have several consequences: first, reducing the level of glial depolarization in response to local neuronal activation (Hosli *et al.*, 1981), which in turn may affect downstream effects of glial activation, such as the release of ATP, glutamate, and other neuroactive substances (Tian *et al.*, 2005; Fellin *et al.*, 2006; Gomez-Gonzalo *et al.*, 2010; Baird-Daniel *et al.*, 2017); and second, reducing the buffering of local extracellular K^+ by glia, meaning that extracellular K^+ transients in 4-AP will be greater, for a given level of neuronal network activation. Interestingly, Mg^{2+} ions have been shown to block glial Kir4.1 channels under depolarized conditions

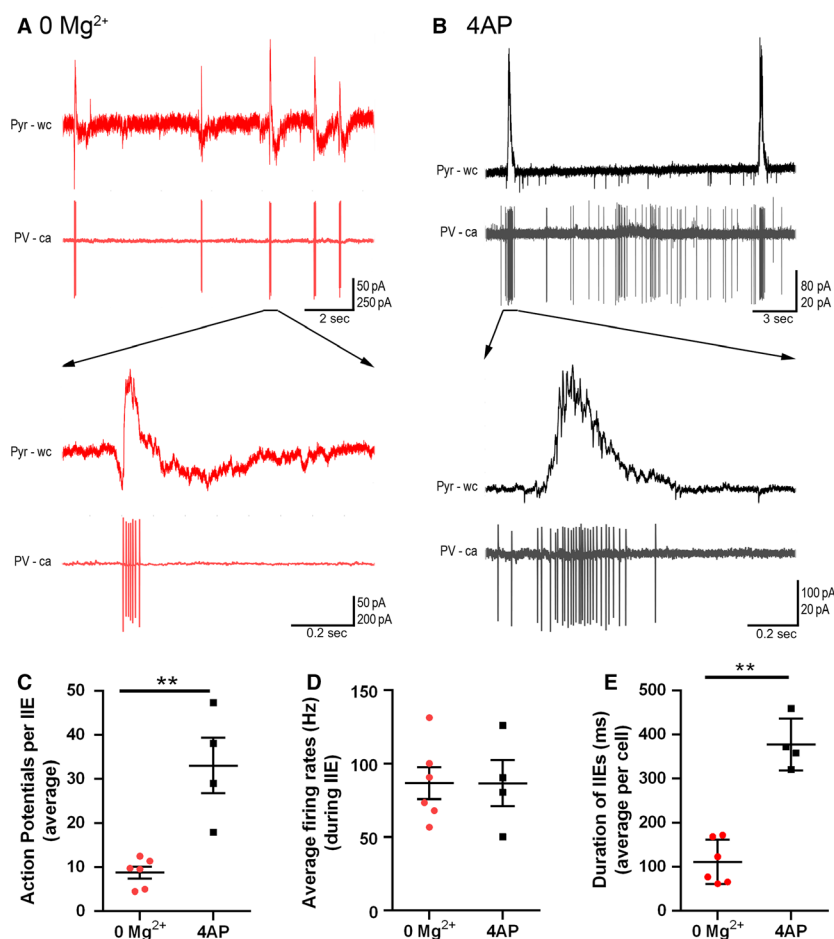


Figure 7. PV firing during interictal events is more sustained in 4AP than in 0 Mg²⁺ events. (A) Example paired recordings of pyramidal cells ("Pyr", recorded in whole cell ("wc") voltage-clamp mode at -30 mV) and PV interneurons (recorded in cell-attached ("ca") mode) in 0 Mg²⁺. Note the intense bursts of PV firing coincident with upwards deflections of the pyramidal trace, consistent with the PV activity being the source of the GABAergic synaptic barrages. (B) Equivalent example paired recordings in 100 μ mol/L 4AP. (C) PV interneurons fire significantly more action potentials per interictal event in 4AP than they do in 0 Mg²⁺ (79 events from six slices analyzed from the 0 Mg²⁺ paradigm while 57 events from four slices were analyzed for the 4AP model; Mann-Whitney test, $**P = 0.0095$). (D) There is no difference in the PV cell firing rates during interictal events between the models. (E) Duration of interictal events are longer in the 4AP model than in 0 Mg²⁺ model (Mann-Whitney test, $**P = 0.0095$).

(Heuser et al., 2014; Olsen et al., 2015), meaning that the 0 Mg²⁺ may be expected to have the opposite effects on glial, instead, enhancing K⁺ buffering by glia, increasing their depolarization, and increasing the downstream effects of glial activation. Indeed, similar to 4AP, the 0 Mg²⁺ model has been demonstrated to influence glial cell neurotransmitter release (Tian et al., 2005). It is, therefore, easy to imagine that glial dysfunction in both models can contribute to some aspects of the induced pathophysiology, but as with the neuronal differences we enumerate, these may not be equivalent in the two models.

These varied differences between the experimental models provide a powerful research tool for investigating

epileptic phenotypes or drug actions in rodent tissue. In transgenic mice carrying mutations associated with epilepsy, it can often be hard to fathom exactly where in the network the problem arises. These acute models though provide a means of "stress-testing" the network (Parrish and Trevelyan, 2018), which may help highlight, for instance, whether the problem is primarily neocortical or hippocampal in origin, or to what extent it involves interneuronal dysfunction, and in what way.

A key lesson from these studies is that superficial similarities between epileptiform activity patterns, especially when viewed only using analyses of field potentials, can conceal important differences in the underlying cellular and network activity. This is of obvious clinical

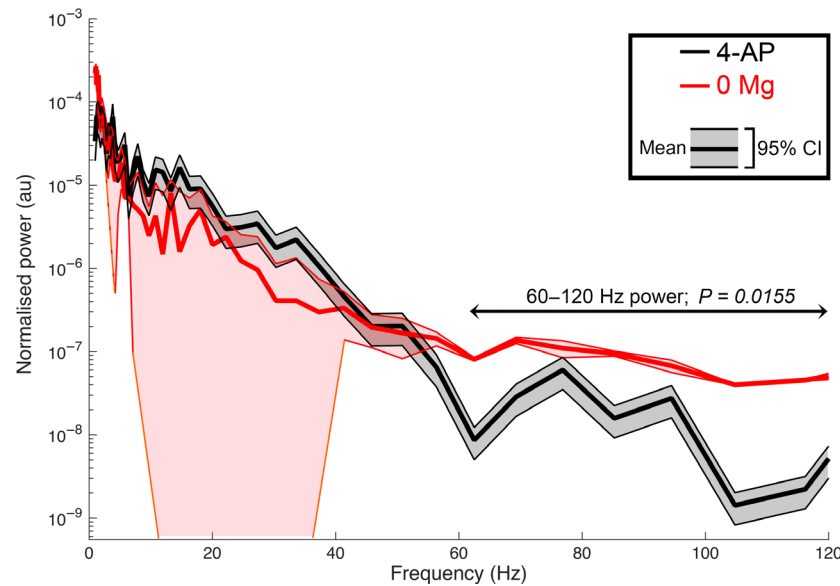


Figure 8. 0 Mg^{2+} and 4AP SLEs differ in higher frequency power. 0 Mg^{2+} seizures display more power in the higher frequency range than 4AP seizures (mean summed power 60–120 Hz (normalized traces), 0 Mg^{2+} = $7.08e-7 \pm 8.99e-7$; 4-AP = $1.78e-7 \pm 4.21e-7$; $P = 0.0155$; 22 and 24 brain slices, respectively). CI, confidence interval.

importance, since field potentials, most of which are not even “local,” but rather surface or scalp EEG, are the only clinical electrophysiological recordings available to us. That is not to say such recordings are worthless, because they clearly do contain huge amounts of information, but we still have much to learn about how to access this for clinical use.

A major motivation behind our study was the important work elucidating ictogenesis in the 4AP model, aided by the development of optogenetic strategies for uniquely activating, or suppressing activity in, specific subpopulations of neurons. Both techniques are compatible with *in vivo* studies, resulting in a large upsurge in the use of 4AP to induce epileptiform activity acutely. It is important therefore to understand how this model gives rise to seizure-like activity, and further, what commonalities, or differences, exist between this model and others. A growing consensus points to a critical role for short-term ionic plasticity affecting particularly fast GABAergic synaptic function (reviewed in (Raimondo *et al.*, 2015), but see also (Thompson and Gahwiler, 1989; Isomura *et al.*, 2003; Viitanen *et al.*, 2010; Ellender *et al.*, 2014). This is exacerbated by other causes of raised intracellular chloride, more chronically (Huberfeld *et al.*, 2007; Dzhalal *et al.*, 2010). On this background of raised $[Cl^-]_i$, bursts of interneuronal activity will excite the most extreme loaded pyramidal cells (Fujiwara-Tsukamoto *et al.*, 2010), and will further load other cells with chloride acutely. Moreover, this raised intracellular Cl^- then causes a secondary surge in extracellular $[K^+]_o$, due to coupled

extrusion of Cl^- and K^+ mediated by KCC2 (Viitanen *et al.*, 2010).

Specific optogenetic activation of interneurons has been shown to trigger SLEs, albeit not invariably, in 4AP (Ledri *et al.*, 2014; Shiri *et al.*, 2015; Yekhlef *et al.*, 2015; Chang *et al.*, 2018) and in the LRD phase of the 0 Mg^{2+} model (Chang *et al.*, 2018). Critically, though, this does not occur early in the 0 Mg^{2+} model (Chang *et al.*, 2019), when SLEs still occur, when GABAergic function remains inhibitory and exercises a marked restraint on propagating epileptiform discharges (Trevelyan *et al.*, 2006). This restraint is powerful, but also short-lived (Trevelyan *et al.*, 2006; Schevon *et al.*, 2012; Ellender *et al.*, 2014), since its enactment provides one of the most rapid means of driving Cl^- into neurons, on account of the massive, and concurrent, GABAergic and glutamatergic synaptic drive (Schevon *et al.*, 2012; Trevelyan and Schevon, 2013; Ellender *et al.*, 2014; Trevelyan *et al.*, 2015; Trevelyan, 2016). Thus, these early SLEs in the 0 Mg^{2+} also involve a progressively compromised GABAergic function arising from short-term ionic plasticity. This then is the nub of the difference between the two models, that in the absence of appreciable glutamatergic drive, spontaneous or induced interneuronal activity can trigger SLEs through an extreme form of GABAergic dysfunction, involving raised intracellular Cl^- and extracellular K^+ . Notably, a recent study of an acute, *in vivo* model, triggered by direct injection of pilocarpine into neocortex, showed the rapid switch, occurring over a few seconds, of the inhibitory effect of PV-interneuron

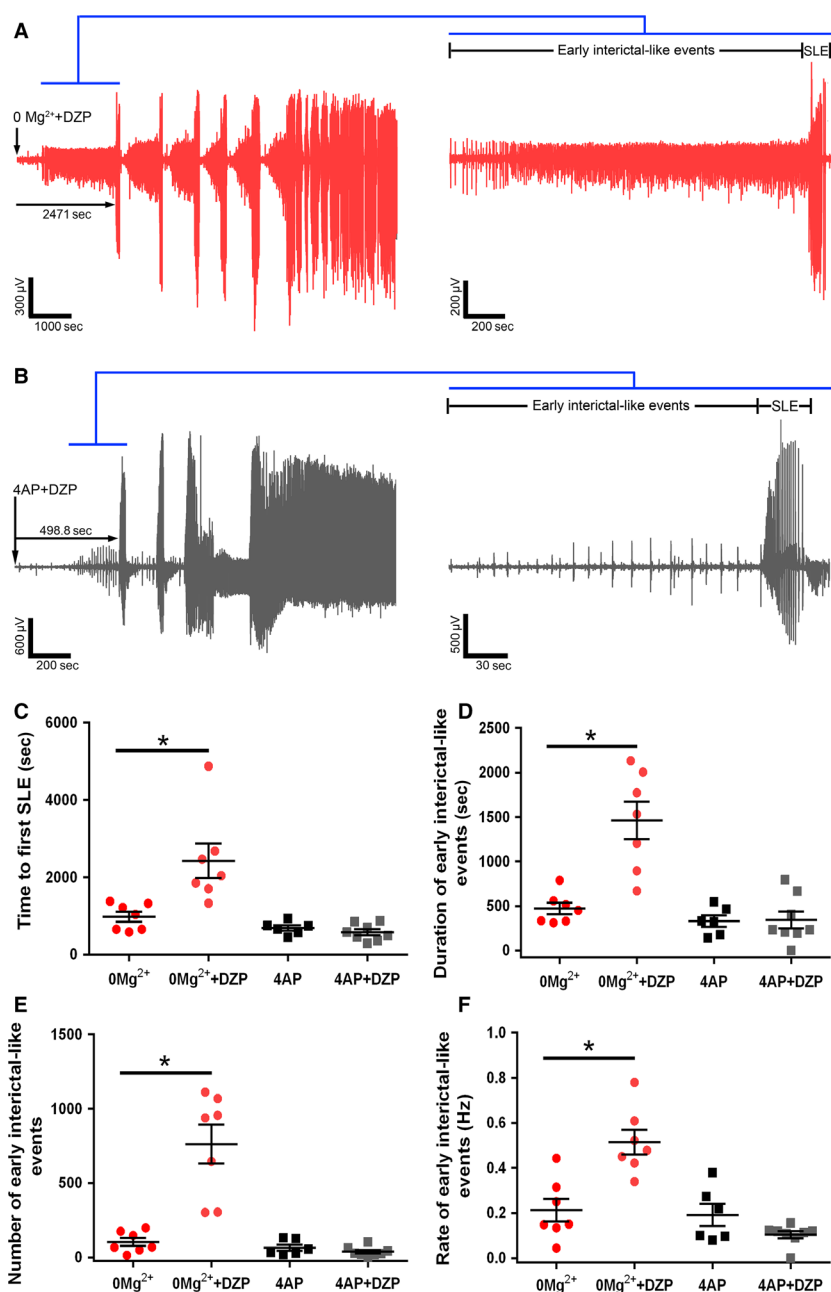


Figure 9. 0 Mg²⁺ model and the 4AP model differ in their sensitivity to diazepam. (A) Representative LFP trace demonstrating the effect of diazepam on 0 Mg²⁺ induced epileptiform activity. (B) Equivalent recording in 4AP. (C) Diazepam significantly delays seizure-like events in the 0 Mg²⁺ model while it has no effect on 4AP induced seizures (ANOVA with post hoc test, **P* = 0.001). (D) Diazepam significantly increases the duration of the early interictal period in the 0 Mg²⁺ model while having no effect in 4AP (ANOVA with post hoc test, **P* = 0.001). (E) Diazepam significantly increases the number of early interictal-like events in the 0 Mg²⁺ model while this remains unchanged in the 4AP (ANOVA with post hoc test, **P* = 0.001). (F) Diazepam significantly increases the rate of early interictal-like events in the 0 Mg²⁺ model while having no effect on the 4AP induced early interictal-like events (ANOVA with post hoc test, **P* = 0.001).

activation to an excitatory one (Magloire et al., 2019), consistent with the previous demonstration in organotypic cultures (Ellender et al., 2014). They further showed that this GABAergic switch could be prevented

by over-expressing KCC2 artificially (introduced by viral vectors), providing strong support for the hypothesized role of short-term ionic plasticity in ictogenesis (Magloire et al., 2019).

Critically, though, in the presence of large glutamatergic drives, ictal recruitment will occur at a far earlier stage in this spectrum of GABAergic dysfunction. It remains an open question for clinical practice which of these two situations is dominant, but one can conceive examples of both. For instance, sensory-triggered seizures, and secondary generalization into cortical areas that had been functioning normally, are both likely to represent cases where the glutamatergic drive is predominant. Optogenetic stimulation of interneurons is an important experimental model, but the key clinical question is whether there are pathological conditions in which one sees spontaneous bursting of interneurons, in the absence of any significant glutamatergic drive. Of course, there could be special clinical cases of this, for instance, such as with genetic mutations of certain classes of K^+ channels that are expressed predominantly in interneurons (Browne *et al.*, 1994; Eunson *et al.*, 2000; Muona *et al.*, 2015). Any EEG marker of such activity would represent an important means of identifying patients at high risk of having a seizure. Furthermore, a clinical understanding of the source of the epileptiform discharges (presence or absence of appreciable glutamatergic drive) is likely to have relevance for determining the most appropriate pharmacological interventions for individual patients.

Acknowledgments

We thank Meribeth Parrish and Claudia Racca for comments on the manuscript.

Conflict of Interests

The authors declare no conflict of interest.

References

- Anderson, W. W., D. V. Lewis, H. S. Swartzwelder, and W. A. Wilson. 1986. Magnesium-free medium activates seizure-like events in the rat hippocampal slice. *Brain Res.* 398:215–219.
- Avoli, M., M. D'Antuono, J. Louvel, R. Kohling, G. Biagini, R. Pumain, *et al.* 2002. Network and pharmacological mechanisms leading to epileptiform synchronization in the limbic system *in vitro*. *Prog. Neurobiol.* 68:167–207.
- Baird-Daniel, E., A. G. S. Daniel, M. Wenzel, D. Li, J. Y. Liou, P. Laffont, *et al.* 2017. Glial calcium waves are triggered by seizure activity and not essential for initiating ictal onset or neurovascular coupling. *Cereb Cortex* 27:3318–3330.
- Bohannon, A. S., and J. J. Hablitz. 2018. Optogenetic dissection of roles of specific cortical interneuron subtypes in GABAergic network synchronization. *J. Physiol.* 596:901–919.
- Bordey, A., and H. Sontheimer. 1999. Differential inhibition of glial $K(+)$ currents by 4-AP. *J. Neurophysiol.* 82:3476–3487.
- Browne, D. L., S. T. Gancher, J. G. Nutt, E. R. Brunt, E. A. Smith, P. Kramer, *et al.* 1994. Episodic ataxia/myokymia syndrome is associated with point mutations in the human potassium channel gene, *KCNA1*. *Nat. Genet.* 8:136–140.
- Buckle, P. J., and H. L. Haas. 1982. Enhancement of synaptic transmission by 4-aminopyridine in hippocampal slices of the rat. *J. Physiol.* 326:109–122.
- Burman, R. J., A. Calin, N. K. Codadu, R. Wright, S. E. Newey, E. van den Berg, *et al.* 2019. Excitatory GABAergic signalling is associated with acquired benzodiazepine resistance in status epilepticus. *Brain*. (In press).
- Chang, W. P., J. J. Wu, and B. C. Shyu. 2013. Thalamic modulation of cingulate seizure activity via the regulation of gap junctions in mice thalamocingulate slice. *PLoS ONE* 8: e62952.
- Chang, M., J. A. Dian, S. Dufour, L. Wang, H. Moradi Chameh, M. Ramani, *et al.* 2018. Brief activation of GABAergic interneurons initiates the transition to ictal events through post-inhibitory rebound excitation. *Neurobiol. Dis.* 109:102–116.
- Chang, M., S. Dufour, P. L. Carlen, and T. A. Valiante. 2019. Generation and on-demand initiation of acute ictal activity in rodent and human tissue. *J Vis Exp.* (143):e57952. <https://www.doi.org/10.3791/57952>
- Codadu, N. K., R. R. Parrish, and A. J. Trevelyan. 2019. Region-specific differences and areal interactions underlying transitions in epileptiform activity. *J. Physiol.* 597:2079–2096.
- de Curtis, M., L. Librizzi, L. Uva, and V. Gnatkovsky. 2019. GABAA receptor-mediated networks during focal seizure onset and progression *in vitro*. *Neurobiol. Dis.* 125:190–197.
- Dreier, J. P., and U. Heinemann. 1991. Regional and time dependent variations of low Mg^{2+} induced epileptiform activity in rat temporal cortex slices. *Exp. Brain Res.* 87:581–596.
- Dreier, J. P., C. L. Zhang, and U. Heinemann. 1998. Phenytoin, phenobarbital, and midazolam fail to stop status epilepticus-like activity induced by low magnesium in rat entorhinal slices, but can prevent its development. *Acta Neurol. Scand.* 98:154–160.
- Dzhala, V. I., K. V. Kuchibhotla, J. C. Glykys, K. T. Kahle, W. B. Swiercz, G. Feng, *et al.* 2010. Progressive NKCC1-dependent neuronal chloride accumulation during neonatal seizures. *J. Neurosci.* 30:11745–11761.
- Ellender, T. J., J. V. Raimondo, A. Irkle, K. P. Lamsa, and C. J. Akerman. 2014. Excitatory effects of parvalbumin-expressing interneurons maintain hippocampal epileptiform activity via synchronous afterdischarges. *J. Neurosci.* 34:15208–15222.
- Eunson, L. H., R. Rea, S. M. Zuberi, S. Youroukos, C. P. Panayiotopoulos, R. Liguori, *et al.* 2000. Clinical, genetic, and expression studies of mutations in the potassium channel gene *KCNA1* reveal new phenotypic variability. *Ann. Neurol.* 48:647–656.

- Fellin, T., M. Gomez-Gonzalo, S. Gobbo, G. Carmignoto, and P. G. Haydon. 2006. Astrocytic glutamate is not necessary for the generation of epileptiform neuronal activity in hippocampal slices. *J. Neurosci.* 26:9312–9322.
- Frangoso-Veloz, J., and R. Tapia. 1992. NMDA receptor antagonists protect against seizures and wet-dog shakes induced by 4-aminopyridine. *Eur. J. Pharmacol.* 221:275–280.
- Fujiwara-Tsukamoto, Y., Y. Isomura, M. Imanishi, T. Ninomiya, M. Tsukada, Y. Yanagawa, et al. 2010. Prototypic seizure activity driven by mature hippocampal fast-spiking interneurons. *J. Neurosci.* 30:13679–13689.
- Gomez-Gonzalo, M., G. Losi, A. Chiavegato, M. Zonta, M. Cammarota, M. Brondi, et al. 2010. An excitatory loop with astrocytes contributes to drive neurons to seizure threshold. *Plos Biol.* 8:e1000352.
- Gonzalez, O. C., Z. Shiri, G. P. Krishnan, T. L. Myers, S. Williams, M. Avoli, et al. 2018. Role of KCC2-dependent potassium efflux in 4-Aminopyridine-induced Epileptiform synchronization. *Neurobiol. Dis.* 109:137–147.
- Goodkin, H. P., J. L. Yeh, and J. Kapur. 2005. Status epilepticus increases the intracellular accumulation of GABAA receptors. *J. Neurosci.* 25:5511–5520.
- Heuser, K., K. Szokol, and E. Tauboll. 2014. The role of glial cells in epilepsy. *Tidsskr Nor Laegeforen* 134:37–41.
- Hosli, L., E. Hosli, P. F. Andres, and H. Landolt. 1981. Evidence that the depolarization of glial cells by inhibitory amino acids is caused by an efflux of K⁺ from neurones. *Exp Brain Res* 42:43–48.
- Huberfeld, G., L. Wittner, S. Clemenceau, M. Baulac, K. Kaila, R. Miles, et al. 2007. Perturbed chloride homeostasis and GABAergic signaling in human temporal lobe epilepsy. *J. Neurosci.* 27:9866–9873.
- Isomura, Y., M. Sugimoto, Y. Fujiwara-Tsukamoto, S. Yamamoto-Muraki, J. Yamada, and A. Fukuda. 2003. Synaptically activated Cl⁻ accumulation responsible for depolarizing GABAergic responses in mature hippocampal neurons. *J. Neurophysiol.* 90:2752–2756.
- Jacoby, A., and G. A. Baker. 2008. Quality-of-life trajectories in epilepsy: a review of the literature. *Epilepsy Behav.* 12:557–571.
- Kapur, J., and R. L. Macdonald. 1997. Rapid seizure-induced reduction of benzodiazepine and Zn²⁺ sensitivity of hippocampal dentate granule cell GABAA receptors. *J. Neurosci.* 17:7532–7540.
- Ledri, M., M. G. Madsen, L. Nikitidou, D. Kirik, and M. Kokaia. 2014. Global optogenetic activation of inhibitory interneurons during epileptiform activity. *J. Neurosci.* 34:3364–3377.
- Levesque, M., P. Salami, C. Behr, and M. Avoli. 2013. Temporal lobe epileptiform activity following systemic administration of 4-aminopyridine in rats. *Epilepsia* 54:596–604.
- Magloire, V., M. S. Mercier, D. M. Kullmann, and I. Pavlov. 2018. GABAergic Interneurons in Seizures: Investigating Causality With Optogenetics. *Neuroscientist* 1073858418805002.
- Magloire, V., J. Cornford, A. Lieb, D. M. Kullmann, and I. Pavlov. 2019. KCC2 overexpression prevents the paradoxical seizure-promoting action of somatic inhibition. *Nat. Commun.* 10:1225.
- Manjarrez-Marmolejo, J., and J. Franco-Perez. 2016. Gap junction blockers: an overview of their effects on induced seizures in animal models. *Curr. Neuropharmacol.* 14:759–771.
- Martin, E. D., and M. A. Pozo. 2003. Valproate suppresses status epilepticus induced by 4-aminopyridine in CA1 hippocampus region. *Epilepsia* 44:1375–1379.
- Mayer, M. L., G. L. Westbrook, and P. B. Guthrie. 1984. Voltage-dependent block by Mg²⁺ of NMDA responses in spinal cord neurones. *Nature* 309:261–263.
- Miles, R., and R. K. Wong. 1983. Single neurones can initiate synchronized population discharge in the hippocampus. *Nature* 306:371–373.
- Mitterdorfer, J., and B. P. Bean. 2002. Potassium currents during the action potential of hippocampal CA3 neurons. *J. Neurosci.* 22:10106–10115.
- Mody, I., J. D. Lambert, and U. Heinemann. 1987. Low extracellular magnesium induces epileptiform activity and spreading depression in rat hippocampal slices. *J. Neurophysiol.* 57:869–888.
- Muona, M., S. F. Berkovic, L. M. Dibbens, K. L. Oliver, S. Maljevic, M. A. Bayly, et al. 2015. A recurrent de novo mutation in KCNC1 causes progressive myoclonus epilepsy. *Nat. Genet.* 47:39–46.
- Olsen, M. L., B. S. Khakh, S. N. Skatchkov, M. Zhou, C. J. Lee, and N. Rouach. 2015. New insights on astrocyte ion channels: critical for homeostasis and neuron-glia signaling. *J. Neurosci.* 35:13827–13835.
- Parrish, R. R., and A. J. Trevelyan. 2018. Stress-testing the brain to understand its breaking points. *J. Physiol.* 596:2033–2034.
- Parrish, R. R., N. K. Codadu, C. Racca, and A. J. Trevelyan. 2018. Pyramidal cell activity levels affect the polarity of activity-induced gene transcription changes in interneurons. *J. Neurophysiol.* 120:2358–2367.
- Parrish, R. R., N. K. Codadu, C. M. Scott, and A. J. Trevelyan. 2019. Feedforward inhibition ahead of ictal wavefronts is provided by both parvalbumin and somatostatin expressing interneurons. *J. Physiol.* 597(8):2297–2314.
- Raimondo, J. V., R. J. Burman, A. A. Katz, and C. J. Akerman. 2015. Ion dynamics during seizures. *Front. Cell. Neurosci.* 9:419.
- Rutecki, P. A., F. J. Lebeda, and D. Johnston. 1987. 4-Aminopyridine produces epileptiform activity in hippocampus and enhances synaptic excitation and inhibition. *J. Neurophysiol.* 57:1911–1924.
- Schevon, C. A., S. A. Weiss, G. Jr McKhann, R. R. Goodman, R. Yuste, R. G. Emerson, et al. 2012. Evidence of an

- inhibitory restraint of seizure activity in humans. *Nat. Commun.* 3:1060.
- Schevon, C. A., S. Tobochnik, T. Eissa, E. Merricks, B. Gill, R. R. Parrish, et al. 2019. Multiscale recordings reveal the dynamic spatial structure of human seizures. *Neurobiology Dis.* 127:303–311.
- Shiri, Z., F. Manseau, M. Levesque, S. Williams, and M. Avoli. 2015. Interneuron activity leads to initiation of low-voltage fast-onset seizures. *Ann Neurol.* 77:541–546.
- Sirven, J. I. 2015. Epilepsy: a spectrum disorder. *Cold Spring Harb. Perspect. Med.* 5:a022848.
- Thompson, S. M., and B. H. Gähwiler. 1989. Activity-dependent disinhibition. I. Repetitive stimulation reduces IPSP driving force and conductance in the hippocampus in vitro. *J. Neurophysiol.* 61:501–511.
- Tian, G. F., H. Azmi, T. Takano, Q. Xu, W. Peng, J. Lin, et al. 2005. An astrocytic basis of epilepsy. *Nat. Med.* 11:973–981.
- Traub, R. D., and R. Miles. 1991. *Neuronal networks of the hippocampus*. Cambridge University Press, Cambridge, UK.
- Trevelyan, A. J. 2016. Do cortical circuits need protecting from themselves? *Trends Neurosci* 39:502–511.
- Trevelyan, A. J., and C. A. Schevon. 2013. How inhibition influences seizure propagation. *Neuropharmacology* 69:45–54.
- Trevelyan, A. J., D. Sussillo, B. O. Watson, and R. Yuste. 2006. Modular propagation of epileptiform activity: evidence for an inhibitory veto in neocortex. *J. Neurosci.* 26:12447–12455.
- Trevelyan, A. J., D. Sussillo, and R. Yuste. 2007. Feedforward inhibition contributes to the control of epileptiform propagation speed. *J. Neurosci.* 27:3383–3387.
- Trevelyan, A. J., S. F. Muldoon, E. M. Merricks, C. Racca, and K. J. Staley. 2015. The role of inhibition in epileptic networks. *J. Clin. Neurophysiol.* 32:227–234.
- Viitanen, T., E. Ruusuvaari, K. Kaila, and J. Voipio. 2010. The K⁺-Cl⁻ cotransporter KCC2 promotes GABAergic excitation in the mature rat hippocampus. *J. Physiol.* 588:1527–1540.
- Voss, L. J., G. Jacobson, J. W. Sleight, A. Steyn-Ross, and M. Steyn-Ross. 2009. Excitatory effects of gap junction blockers on cerebral cortex seizure-like activity in rats and mice. *Epilepsia* 50:1971–1978.
- Williams, S. B., and J. J. Hablitz. 2015. Differential modulation of repetitive firing and synchronous network activity in neocortical interneurons by inhibition of A-type K(+) channels and I_h. *Front. Cell. Neurosci.* 9:89.
- Wong, B. Y., and D. A. Prince. 1990. The lateral spread of ictal discharges in neocortical brain slices. *Epilepsy Res.* 7:29–39.
- Yekhlief, L., G. L. Breschi, L. Lagostena, G. Russo, and S. Taverna. 2015. Selective activation of parvalbumin- or somatostatin-expressing interneurons triggers epileptic seizurelike activity in mouse medial entorhinal cortex. *J. Neurophysiol.* 113:1616–1630.